Title

A Whole-Genome RNA Interference Screen Reveals a Role for *Spry2* in Insulin Transcription and the Unfolded Protein Response.

Journal

Diabetes, 66(6)

ISSN

0012-1797

Authors

Pappalardo, Zachary
Gambhir Chopra, Deeksha
Hennings, Thomas G
et al.

Publication Date

2017-06-01

DOI

10.2337/db16-0962

Peer reviewed

A Whole-Genome RNA Interference Screen Reveals a Role for *Spry2* in Insulin Transcription and the Unfolded Protein Response

Zachary Pappalardo,[1] Deeksha Gambhir Chopra,[1] Thomas G. Hennings,[1,2] Hunter Richards,[1] Justin Choe,[1] Katherine Yang,[1] Luc Baeyens,[1] Kenny Ang,[3] Steven Chen,[3] Michelle Arkin,[3] Michael S. German,[1,4] Michael T. McManus,[1,5] and Gregory M. Ku[1,4]

Diabetes 2017;66:1703–1712 | https://doi.org/10.2337/db16-0962

Insulin production by the pancreatic β-cell is required for normal glucose homeostasis. While key transcription factors that bind to the insulin promoter are known, relatively little is known about the upstream regulators of insulin transcription. Using a whole-genome RNA interference screen, we uncovered 26 novel regulators of insulin transcription that regulate diverse processes including oxidative phosphorylation, vesicle traffic, and the unfolded protein response (UPR). We focused on *Spry2*—a gene implicated in human type 2 diabetes by genome-wide association studies but without a clear connection to glucose homeostasis. We showed that *Spry2* is a novel UPR target and its upregulation is dependent on PERK. Knockdown of *Spry2* resulted in reduced expression of Serca2, reduced endoplasmic reticulum calcium levels, and induction of the UPR. *Spry2* deletion in the adult mouse β-cell caused hyperglycemia and hypoinsulinemia. Our study greatly expands the compendium of insulin promoter regulators and demonstrates a novel β-cell link between *Spry2* and human diabetes.

Worldwide, 354 million people have diabetes, and this is projected to increase to 592 million by the year 2035 (1). The majority of this rise will be in type 2 diabetes, although the incidence of type 1 diabetes also continues to rise (2,3). The pathophysiological common ground of diabetes is β-cell dysfunction and loss. Genome-wide association studies of patients with type 2 diabetes have identified approximately eighty risk loci, many of which are located near genes that would be predicted to affect β-cell function (reviewed by Morris [4]). However, only a few of the identified single nucleotide polymorphisms (SNPs) have been experimentally verified to work through the genes to which they have been assigned. We hypothesized that augmenting current genome-wide association studies results with unbiased screens for the genes that control normal β-cell function would reveal novel targets for future diabetes therapeutics and generate a more complete picture of the genes involved in the pathogenesis of human diabetes.

We performed a whole-genome RNA interference (RNAi) screen for regulators of the human insulin promoter. We identified novel regulators of insulin production including a type 2 diabetes locus, *Spry2* (5–7). *Spry2* is known to negatively regulate growth factor signaling, but its link to diabetes is not clear. We discovered a novel role for *Spry2* in the unfolded protein response (UPR) and established it as a UPR target. Our study provides a blueprint for functionally annotating the β-cell insulin production pathway and reveals a novel mechanism linking *Spry2* to human diabetes.

RESEARCH DESIGN AND METHODS

Cells and RNAi Screen

MIN6 cells were a gift from Dr. J. Miyazaki (Osaka University). The screening MIN6 cell line, containing a lentivirally

[1]Diabetes Center, University of California, San Francisco, San Francisco, CA
[2]Biomedical Sciences Graduate Program, University of California, San Francisco, San Francisco, CA
[3]Small Molecule Discovery Center, University of California, San Francisco, San Francisco, CA
[4]Division of Endocrinology and Metabolism, Department of Medicine, University of California, San Francisco, San Francisco, CA
[5]Department of Microbiology and Immunology, University of California, San Francisco, San Francisco, CA

Corresponding author: Gregory M. Ku, gregory.ku@ucsf.edu.

Received 7 August 2016 and accepted 16 February 2017.

This article contains Supplementary Data online at http://diabetes.diabetesjournals.org/lookup/suppl/doi:10.2337/db16-0962/-/DC1.

See accompanying article, p. 1467.

delivered copy of the human insulin promoter driving EGFP and a distinct integrated copy of the rous sarcoma virus (RSV) promoter driving mCherry, was previously described (8). A total of 1.25 pmol of each small interfering RNA (siRNA) from the Qiagen Whole Genome Mouse siRNA library version 1.0 was placed individually into wells of 384-well plates. Totals of 0.05 μL of RNAiMax (Life Technologies) and 9.95 μL of Opti-MEM (Life Technologies) followed by 10,000 reporter MIN6 cells in 40 μL of growth media (DMEM high glucose, 10% FBS, penicillin, streptomycin) were added to each well. Five days after transfection, fluorescence was read using an Analyst HT (Molecular Devices). GFP fluorescence was divided by mCherry fluorescence. Wells with mCherry fluorescence 1.5 SD below the mean of that plate were removed because of presumed cellular toxicity. Scores were median two-way polished to remove edge effects. A subset of the whole-genome library was repeated using 0.5 μL of HiPerFect (Qiagen) and 9.5 μL of Opti-MEM (Life Technologies) per well instead of RNAiMax. Transfection efficiency for both reagents was typically >90%.

Quantitative RT-PCR

Total RNA was prepared with TRIzol Reagent (Life Technologies) followed by DNA digestion with TURBO DNase (Ambion). Oligo-dT– and random hexamer–primed cDNA was synthesized with SuperScript III (Life Technologies). For TaqMan primers, the delta-delta CT method was used using the average CT of β-actin, β-glucuronidase, cyclophilin, and TBP as reference genes. For SYBR Green primers, data were normalized to β-actin. Primer sequences are listed in Supplementary Table 4.

mRNA-Seq

A single RNA isolation from the screening cell line was used to generate a polyA-primed mRNA-Seq library as previously described, except Cufflinks 2.0.2 was used for the fragments per kilobase of transcript per million mapped reads (FPKM) determination (9,10). Reads have been deposited in the National Center for Biotechnology Information Sequence Read Archive (SAMN06250888).

Gene Ontology Term Enrichment

Database for Annotation, Visualization and Integrated Discovery v6.7 was used to find enriched gene ontology (GO) terms (11).

Mice

Spry2 floxed mice were a gift from Dr. O. Klein (University of California, San Francisco). Mouse insulin promoter–CreERT (MIP1-CreERT) mice were a gift from Dr. N. Tamarina (University of Chicago). Mice received three subcutaneous 2-mg tamoxifen injections (Sigma-Aldrich) at 6 weeks of age; each injection was separated by a day. Intraperitoneal glucose tolerance testing was performed at 12 weeks: 2 g/kg glucose was injected into the peritoneal space after a 6-h fast, and blood glucose was monitored with a FreeStyle Lite Glucometer (Abbott). Glucose tolerance *P* values between the three genotypes were calculated using a one-way ANOVA with repeated measures followed by pairwise comparisons corrected with the Benjamini-Hochberg method for multiple testing. The glucose area under the curve above fasting was measured using the trapezoidal method. Insulin tolerance tests were performed at 14 weeks: after a 6-h fast, 0.1 mU/gram body weight of regular insulin was injected into the peritoneal space. Plasma insulin levels were measured at 15 weeks: after a 16-h fast and after a 2 g/kg intraperitoneal glucose injection. Islets were isolated as previously described (12). RNA was harvested with TRIzol 1 day after isolation.

Western Blots

Cells were lysed in buffer containing the following: 50 mmol/L TrisHCl pH 6.7, 150 mmol/L NaCl, 1% Triton X-100, cOmplete Protease Inhibitor Cocktail (Roche), Phosphatase Inhibitor Cocktail 2 (Sigma-Aldrich), and Phosphatase Inhibitor Cocktail 3 (Sigma-Aldrich). The following antibodies were used: anti-Wfs1 (11558–1-AP; Proteintech), phospho-PERK (3179; Cell Signaling), phospho-Eif2α (3398; Cell Signaling), total Eif2α (9722S; Cell Signaling), total PERK (3192S; Cell Signaling), GAPDH (G8795; Sigma-Aldrich), Spry2 (ab50317; Abcam), and Serca2 (sc-8095; Santa Cruz Biotechnology). Islet protein samples were isolated from the TRIzol Reagent organic phase after RNA isolation as described in the protocol, except the pellet was resuspended in 5 mol/L urea in 0.5% SDS.

D1ER Calcium Measurements

Unmodified MIN6 cells were infected with a lentivirus expressing endoplasmic reticulum (ER)-targeted fluorescent cameleon D1ER. If indicated, the cells were transfected with the indicated siRNAs and rested for 5 days prior to analysis. For measurement of ER cells low in calcium, the cells were trypsinized and resuspended in complete media. Flow cytometry was performed using an Attune Cytometer (Life Technologies) using VL2 and VL1 as the fluorescence resonance energy transfer (FRET) emission channel and the CFP (donor) channel, respectively. VL2 was divided by VL1 to calculate the FRET signal. The FRET low population was defined as those having >33% reduction in the FRET signal compared with the geometric mean of the population. FRET low was typically 5–8% of the cell population for the control siRNA transfection.

siRNAs

Anti-luciferase siRNA, AllStars Negative Control siRNA, and Negative Control siRNA were obtained from Qiagen.

Annexin V Staining

Parental MIN6 cells were stained with Annexin V Alexa Fluor 488 & Propidium Iodide (Life Technologies) and analyzed by flow cytometry (Attune; Life Technologies). The percentage of total events that were annexin V positive and propidium iodide negative is shown. For percent cell death, MIN6 cells were trypsinzed and the percentage of events in the live gate determined by forward and side scatter was subtracted from 100%.

Statistics

Unless otherwise specified, *P* values were calculated by two-tailed Student *t* test and corrected for false discovery using the Benjamini-Hochberg method. For quantitation of Western blot bands (phospho-PERK, phospho-Eif2α, Spry2 induction by UPR inducers, Spry2 or Wfs1 knockdown), the log-transformed ratio of the experimental condition to the control condition was used for a one-sample Student *t* test.

RESULTS

Whole-Genome RNAi Screen for Regulators of the Insulin Promoter

To elucidate genes that alter insulin transcription, we previously generated a MIN6 mouse insulinoma clonal cell line that harbors an EGFP reporter driven by the proximal 362 bases of the human insulin promoter. To avoid selecting hits that affect general transcription, this line was engineered to constitutively express a control mCherry reporter driven by the RSV promoter (8). This reporter cell line was used in a high-throughput RNAi screen using a commercial library containing 75,366 unique siRNAs targeting ~22,000 mouse genes with 3–4 unique siRNAs per gene. Each siRNA was individually reverse transfected into the reporter cell line in 384-well plates. Five days after transfection, the ratio of GFP to mCherry fluorescence was measured (Fig. 1*A*). The plate-based assay performance metric Z′ typically ranged from 0.6–0.8 (0.5 is considered acceptable; Supplementary Fig. 1*A*) (13). Gene-level *P* values for positive regulators of insulin expression (reduced GFP/mCherry) were

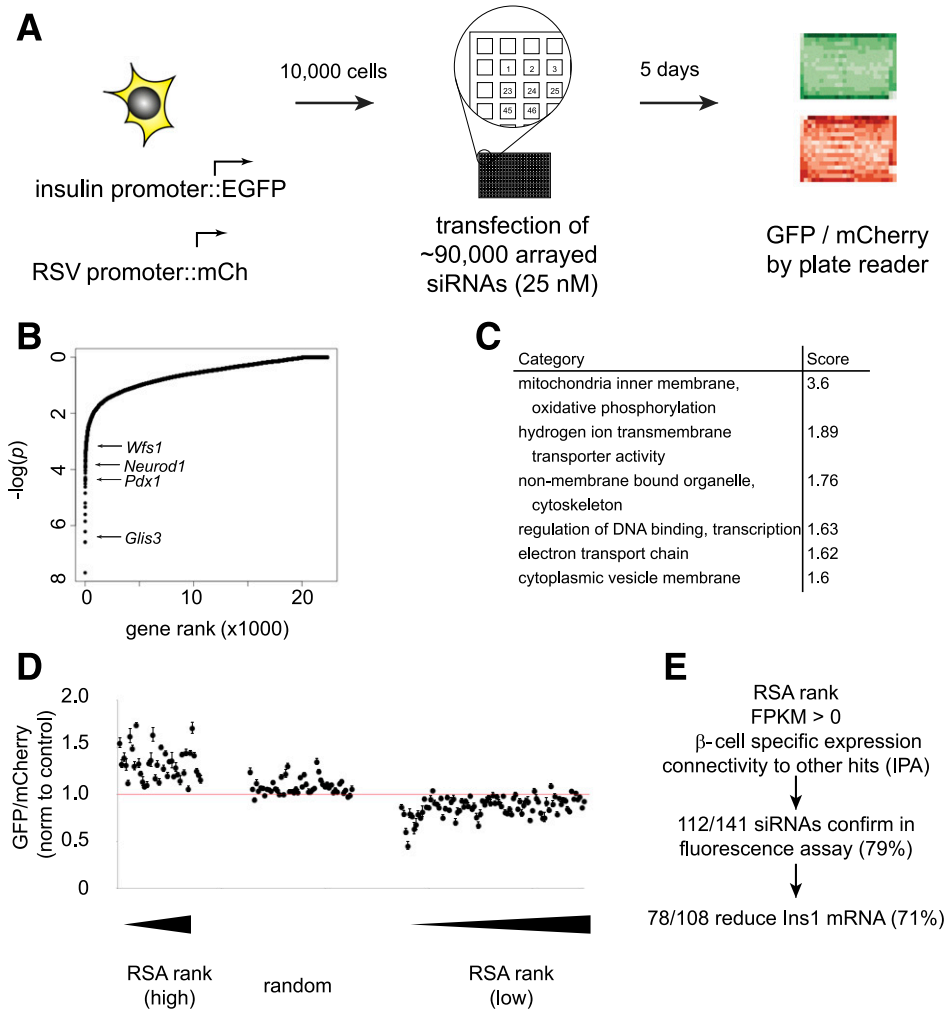

Figure 1—Whole-genome RNAi screen reveals novel regulators of the insulin promoter. *A*: Screen schematic: MIN6 cells expressing EGFP under control of the insulin promoter and mCherry (mCh) under control of the RSV promoter are transfected with siRNAs in 384-well plates, and GFP and mCherry are read out by a plate reader. *B*: −log(p) value for positive regulator genes screened as determined by RSA. *C*: Enriched GO term categories with enrichment scores [−log(p)]. *D*: GFP/mCherry fluorescence for siRNAs during secondary screening normalized (norm) to control anti-luciferase siRNA. Each point represents the GFP/mCherry fluorescence compared with control with SEM. siRNAs are ordered by RSA rank for positive regulators (right cluster), randomly selected from all siRNAs (center cluster), or ordered by RSA rank for negative regulators (left cluster). $n \geq 3$. For FDR-corrected *P* values, see Supplementary Table 2. *E*: Criteria used for selection of siRNAs for secondary screening and overall confirmation rates. IPA, Ingenuity Pathway Analysis.

determined using the redundant siRNA analysis (RSA), where *P* values are assigned based on the number and strength of siRNAs to that gene (14).

A portion of the screen was repeated with an alternative lipid transfection reagent to ensure results were not specific to the transfection reagent used. Normalized scores for each siRNA were well correlated (Supplementary Fig. 1*B*), and gene-level *P* values for positive regulators of insulin transcription were also well correlated (Supplementary Fig. 1*C*). To reduce off-target effects, we did not further consider siRNAs targeting genes that were not expressed using mRNA-Seq of the screening cell line (Supplementary Table 1). As would be expected, the fraction of hits that were not expressed in the screening cell line increased as more inferior hits were considered (Supplementary Fig. 1*D*).

When ranked based on low GFP/mCherry (i.e., specific suppression of insulin expression), the key β-cell transcription factors, *Glis3*, *Pdx1*, and *Neurod1*, were ranked 3rd, 17th, and 29th, respectively (Fig. 1*B*), providing strong validation for the screen. *Wfs1*, a known regulator of both insulin production and insulin secretion, was also identified. GO terms involving mitochondria, DNA transcription, vesicular transport, and cytoskeleton were significantly enriched among the top 300 genes that, when knocked down, reduced GFP/mCherry (Fig. 1*C*).

To validate the primary screen, we retested the top 40 siRNAs targeting putative positive regulators, selecting the top 2–3 performing siRNAs for each gene by GFP/mCherrry reduction. These siRNAs were transfected into the screening cell line in biological triplicate, and GFP and mCherry were measured. Of the top 40 siRNAs targeting putative positive regulators, 36 (90%) reduced GFP/mCherry compared with a control siRNA during retesting. Of 50 random siRNAs selected from the library, only one showed a statistically significant reduction in GFP/mCherry (Fig. 1*D*). We then selected additional siRNAs for retesting based on β-cell expression, interconnectivity (based on GO term enrichment), and published data for a specific role in β-cell function (Fig. 1*E*). In total, 141 siRNAs targeting positive regulators were tested in the screening assay with RSA ranks up to 6,313. A total of 112/141 (79%) showed a statistically significant reduction in GFP/mCherry compared with a control siRNA (Fig. 1*E* and Supplementary Table 2).

As GFP/mCherry fluorescence is a surrogate for insulin promoter activity, siRNAs were tested for their ability to reduce endogenous, unspliced insulin mRNA, as this has a shorter half-life than mature insulin message (15,16). We used a quantitative RT-PCR (qRT-PCR) assay for pre*Ins1* mRNA, as we found that this was more sensitive to *Pdx1, Glis3*, and *NeuroD1* knockdown than pre*Ins2* mRNA (data not shown). A total of 78/108 (72%) siRNAs reduced pre*Ins1* mRNA. We considered genes with two siRNAs showing reduced pre*Ins1* mRNA as high-confidence hits. We found 29 such genes, 26 of which did not have a known role in insulin promoter activity. An additional 15 genes had one of two siRNAs reduce insulin mRNA levels (Fig. 2*A*). With the exception of three genes without a known human ortholog, all of our validated hits are expressed in human islets at reads per kilobase of transcript per million mapped reads (RPKM) >0.1, suggesting that they could play a similar role in insulin production in human β-cells (Supplementary Table 3) (17). Although the screen was not optimized to detect increases in GFP/mCherry, when the siRNAs were ranked according to increased GFP/mCherry (targeting putative negative regulators), the top 40 siRNAs did tend to subtly increase GFP/mCherry during retesting (Fig. 1*D*). However, a low rate of these siRNAs increased pre*Ins1* mRNA (data not shown), so we focused on the positive regulators.

To begin to validate our screen in vivo, we examined global knockout (ko) mice of *Gpr75*, one of the G-protein–coupled receptor hits in the screen. We found that *Gpr75* ko mice were modestly hyperglycemic compared with their wild-type (wt) or heterozygous littermates (Supplementary Fig. 2*A* and *B*), despite being more insulin sensitive and having lower body weight (Supplementary Fig. 2*C* and *D*). Plasma insulin levels were lower before and after a glucose challenge in *Gpr75* ko mice as compared with their wt littermates (Supplementary Fig. 2*E*). Finally, insulin secretion in vitro was also blunted in islets from *Gpr75* ko mice (Supplementary Fig. 2*F*). These data show that our in vitro whole-genome RNAi screen was capable of detecting in vivo regulators of β-cell function.

Spry2 Is a Novel Regulator of β-Cell Insulin Transcription

Among the other novel hits, we were particularly interested in *Spry2* because it has been identified in multiple studies as a type 2 diabetes risk locus (5,7). We first returned to the original confirmation qRT-PCR for pre*Ins1*. Of the two *Spry2* siRNAs initially retested, only Spry2_4 statistically significantly reduced pre*Ins1* mRNA; Spry2_6 had a weaker effect and a false discovery rate (FDR)-adjusted *P* value of 0.13 after three biological replicates (Fig. 2*A* and Supplementary Table 2). Therefore, we tested all three siRNAs targeting *Spry2* that were identified as hits in the primary screen. After nine biological replicates, all three independent siRNAs to *Spry2* statistically significantly reduced pre*Ins1* mRNA levels in MIN6 cells after FDR correction (Fig. 2*B*). All three siRNAs reduced *Spry2* mRNA levels (Supplementary Fig. 3).

Spry2 Is a UPR Target

In many cell types, *Spry2* negatively regulates Ras-MAPK signaling (18). Since MAPK signaling is thought to positively regulate insulin transcription, we sought another mechanism for *Spry2*'s positive influence on insulin production (19). We hypothesized that *Spry2* might play a role in the UPR, as dominant negative *Spry2* expression in the mouse lens has been reported to increase ER stress (20). Furthermore, *SPRY2* was induced in human islets treated with palmitate, which induces ER stress (21).

We first asked whether *Spry2* is induced by established chemical UPR inducers. Exposure of MIN6 cells to the sarcoplasmic/endoplasmic reticulum calcium ATPase (Serca) inhibitor thapsigargan increased *Spry2* mRNA

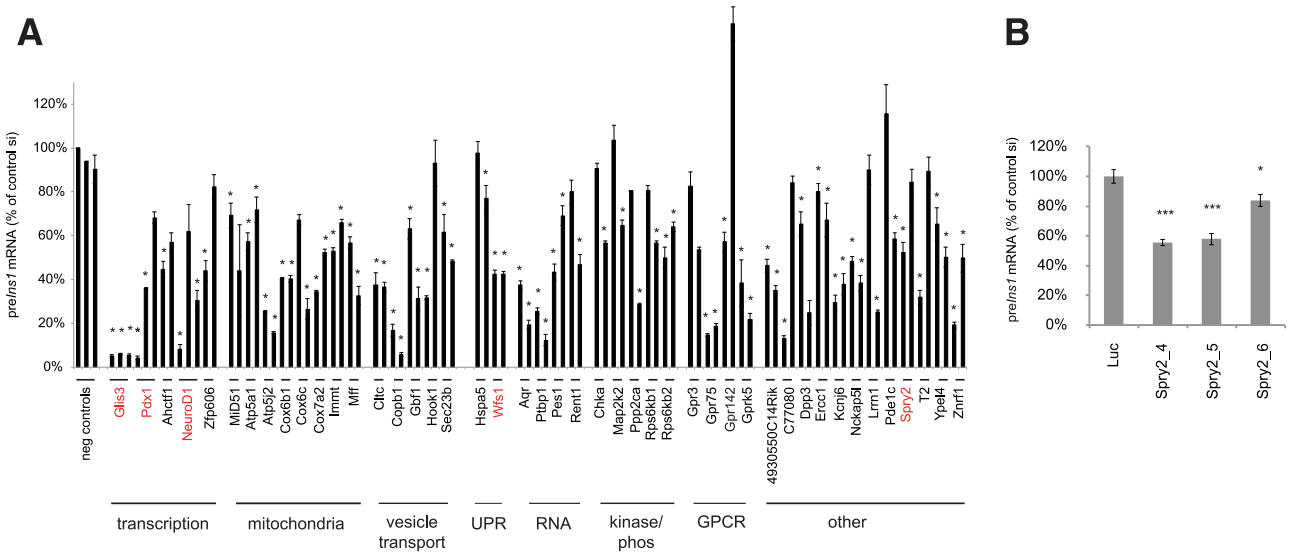

Figure 2—Hit confirmation. *A*: pre*Ins1* mRNA by qRT-PCR with SEM from MIN6 cells transfected with the indicated siRNAs. Red indicates genes known to be involved in human diabetes. *P* values were adjusted for multiple testing using the Benjamini-Hochberg method. For *P* values, see Supplementary Table 2 (n = 3 for each siRNA). Genes are organized according to known functions. *B*: The indicated siRNAs targeting *Spry2* were transfected into MIN6 cells, and pre*Ins1* mRNA was measured by qRT-PCR (n = 9). $^{*}P < 0.05$, $^{***}P < 0.001$. GPCR, G-protein–coupled receptor; neg, negative; phos, phosphatase.

and protein expression (Fig. 3*A* and *B*). The degree of upregulation was similar to that of *Wfs1* mRNA, a gene known to be upregulated by ER stress (22,23). The N-linked glycosylation inhibitor and ER stress inducer tunicamycin also increased *Spry2* mRNA and protein (Supplementary Fig. 4*A* and *B*). Mouse embryonic fibroblasts (MEFs) also upregulated *Spry2* mRNA in response to thapsigargan (Fig. 3*C*) or tunicamycin (Fig. 3*D*). However, MEFs deficient in PERK did not upregulate *Spry2* mRNA in response to thapsigargan or tunicamycin. Finally, since knockdown of *Wfs1* is known to increase ER stress in β-cells, we asked whether knockdown of *Wfs1* might also increase *Spry2* expression in MIN6 cells (24,25). Multiple siRNAs targeting *Wfs1* increased *Spry2* mRNA and Spry2 protein expression in the absence of any other ER stress inducer (Fig. 3*E* and *F*). Notably, these *Wfs1* siRNAs were effective in knockdown of *Wfs1* mRNA (Supplementary Fig. 4*C*) and Wfs1 protein (Supplementary Fig. 4*D*) and in reducing pre*Ins1* mRNA (Supplementary Fig. 4*E*).

Knockdown of *Spry2* Triggers the UPR

Next, we hypothesized that *Spry2* could play a role in regulating the UPR. Knockdown of *Spry2* by multiple independent siRNAs resulted in increased levels of the UPR markers *CHOP* and spliced *Xbp1* (Fig. 4*A* and *B*). BiP expression did not increase after either *Spry2* or *Wfs1* knockdown (data not shown). To further confirm activation of the UPR, we examined the activation of the ER stress sensor PERK and its target Eif2α after siRNA knockdown of *Spry2* or *Wfs1*. Both phospho-PERK and phospho-Eif2α levels increased after either *Spry2* or *Wfs1* knockdown (Fig. 4*C*–*E*). ATF4 and ATF6 levels did not change after *Spry2* knockdown (Supplementary Fig. 5). Since ER stress in β-cells can trigger apoptosis, we measured the frequency of annexin V^+ cells after *Spry2* knockdown. Indeed, knockdown of *Spry2* increased the fraction of annexin V^+ cells (Fig. 4*F*).

Spry2 Affects Serca2 Expression and ER Calcium Levels

Since PERK activation can be triggered by low levels of ER calcium, we measured ER calcium levels using the D1ER cameleon reporter by flow cytometry (26,27). Treatment of D1ER-expressing MIN6 cells with EDTA and ionomycin resulted in an ~60% increase in the number of cells with low levels of FRET, confirming our ability to monitor ER calcium concentrations with D1ER (Supplementary Fig. 6*A* and *B*). When D1ER MIN6 cells were transfected with anti-*Wfs1* siRNAs, there was a 40% increase in ER calcium–low cells, in line with what has been previously reported (26). *Spry2* knockdown by two independent siRNAs also increased the fraction of cells with low levels of ER calcium by 25% (Fig. 5*A*).

Decreased ER calcium could be caused by increased activity of IP3 receptors. However, neither IP1 levels (a breakdown product of IP3) nor expression of PLCγ1, a producer of IP3 that can be regulated by Spry2, changed after *Spry2* knockdown (Supplementary Fig. 6*C* and *D*). Phosphorylated PLCγ1 was not detectable with or without *Spry2* knockdown (data not shown). Therefore, we examined levels of Serca2 after *Spry2* knockdown. Serca2 protein levels were reduced by 50% after *Spry2* knockdown (Fig. 5*B* and *C*), while mRNA levels were not changed (Fig. 5*D*), suggesting posttranscriptional control of Serca2 protein by Spry2.

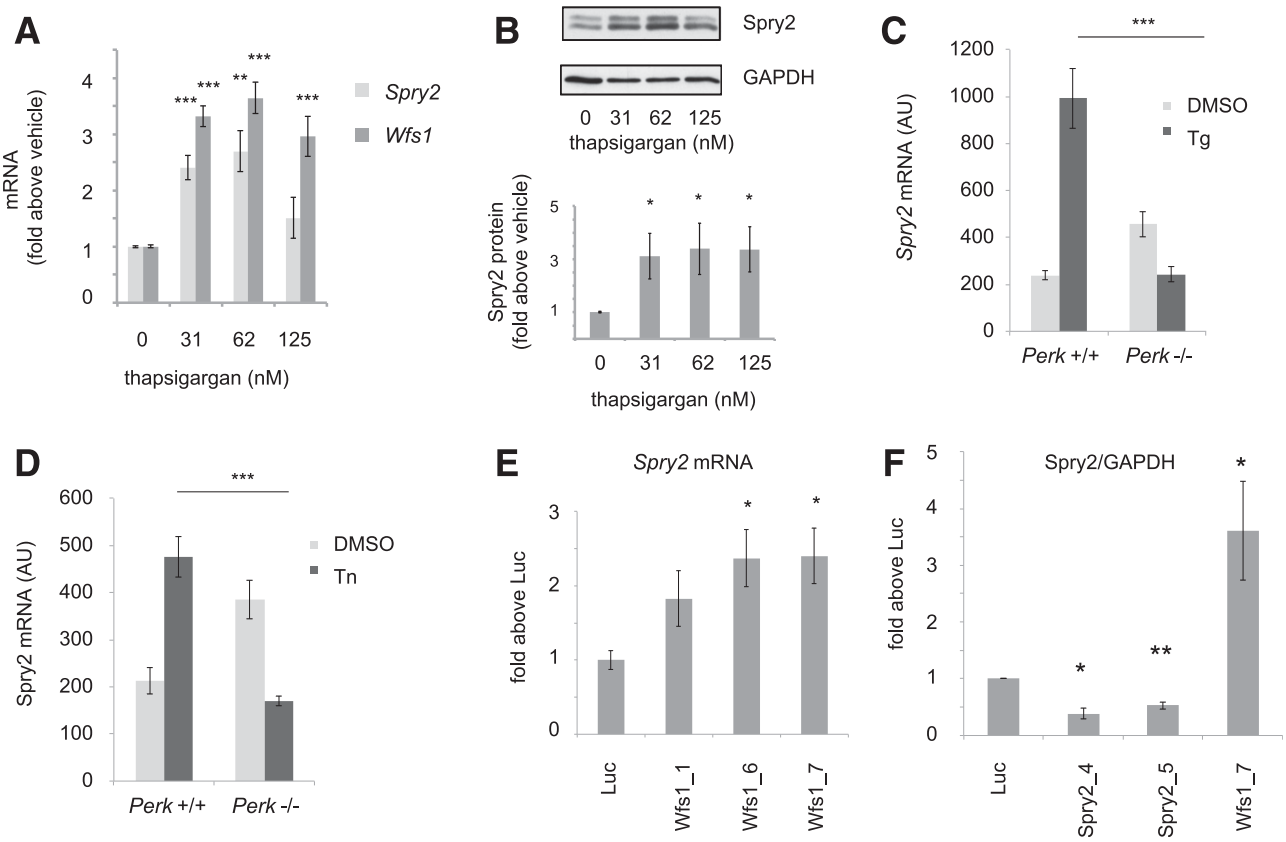

Figure 3—*Spry2* is a UPR target. *A*: MIN6 cells were treated with the indicated concentrations of thapsigargan for 12 h and analyzed for *Spry2* or *Wfs1* expression by qRT-PCR ($n = 6$). *B*: As in *A*, but analyzed for Spry2 protein normalized to GAPDH expression ($n = 4$). *C*: MEFs of the indicated genotype were stimulated with 500 nmol/L thapsigargan (Tg) or vehicle (DMSO) for 6 h and analyzed for *Spry2* expression by qRT-PCR ($n = 6$). *D*: As in *C*, but with 2.5 ug/mL of tunicamycin (Tn). *E*: MIN6 cells were transfected with the indicated siRNA targeting *Wfs1*, and qRT-PCR was performed for *Spry2* mRNA ($n = 9$). *F*: As in *E*, but Spry2 protein was quantitated by Western blot and normalized to GAPDH protein ($n = 3$). For a representative blot, see Fig. 4*C*. SEM is plotted. $^*P < 0.05$, $^{**}P < 0.01$, $^{***}P < 0.001$. AU, arbitrary units.

Alleviating ER Stress Rescues *Spry2*'s Effect on Insulin Production and β-Cell Survival

Since ER stress is known to impact insulin promoter activity, we asked whether amelioration of ER stress could restore insulin production in *Spry2* knockdown cells. Treatment with tauroursodeoxycholic acid (TUDCA) was able to rescue the reduced insulin mRNA seen after *Spry2* knockdown (Fig. 5*E*). Furthermore, TUDCA treatment was able to partially rescue increased β-cell death in MIN6 cells after *Spry2* knockdown (Fig. 5*F*).

β-Cell–Specific Deletion of *Spry2* Results in Hyperglycemia and Hypoinsulinemia

To demonstrate a role for *Spry2* in vivo, we crossed a conditional allele of *Spry2* to MIP1-CreERT mice (28,29) (Fig. 6*A*). Since we were unable to identify a Spry2 antibody suitable for immunohistochemistry, we used droplet digital PCR to measure ko efficiency from islet genomic DNA. Compared with *Spry2* wt/wt MIP1-CreERT mice injected with tamoxifen (*Spry2* wt), there was a 50% reduction in *Spry2* islet genomic DNA in Spry2 flox/flox MIP1-CreERT mice injected with tamoxifen (*Spry2* β-ko) (Supplementary Fig. 7*A*). The heterozygous *Spry2* mice (*Spry2* β-het) showed an intermediate degree of reduction. As ∼70% of the cells from islets are expected to be β-cells, we estimate that the recombination efficiency was approximately 70%. As *Spry2* mRNA is present at approximately twofold higher levels in the mouse α-cell than in the mouse β-cell, we observed a modest but significant reduction in *Spry2* from total islet mRNA of these animals (Supplementary Fig. 7*B*) (30). Protein levels of Spry2 were reduced in *Spry2* β-ko islets compared with *Spry2* β-het islets (Supplementary Fig. 7*C* and *D*).

We asked whether loss of *Spry2* could result in changes in glycemia. After glucose challenge, the *Spry2* β-ko mice were statistically significantly hyperglycemic relative to either *Spry2* wt or *Spry2* β-het mice (Fig. 6*B* and *C*). *Spry2* β-ko mice also had lower plasma insulin levels 15 min after glucose injection (Fig. 6*D*), while their insulin tolerances and weights were not different (Supplementary Fig. 7*E* and *F*). Islets from *Spry2* β-ko mice had slightly lower levels of mature Ins1/2 mRNA, confirming our findings in MIN6 cells (Fig. 6*E*).

Despite lower insulin mRNA levels, total pancreatic insulin content normalized to total protein was not reduced

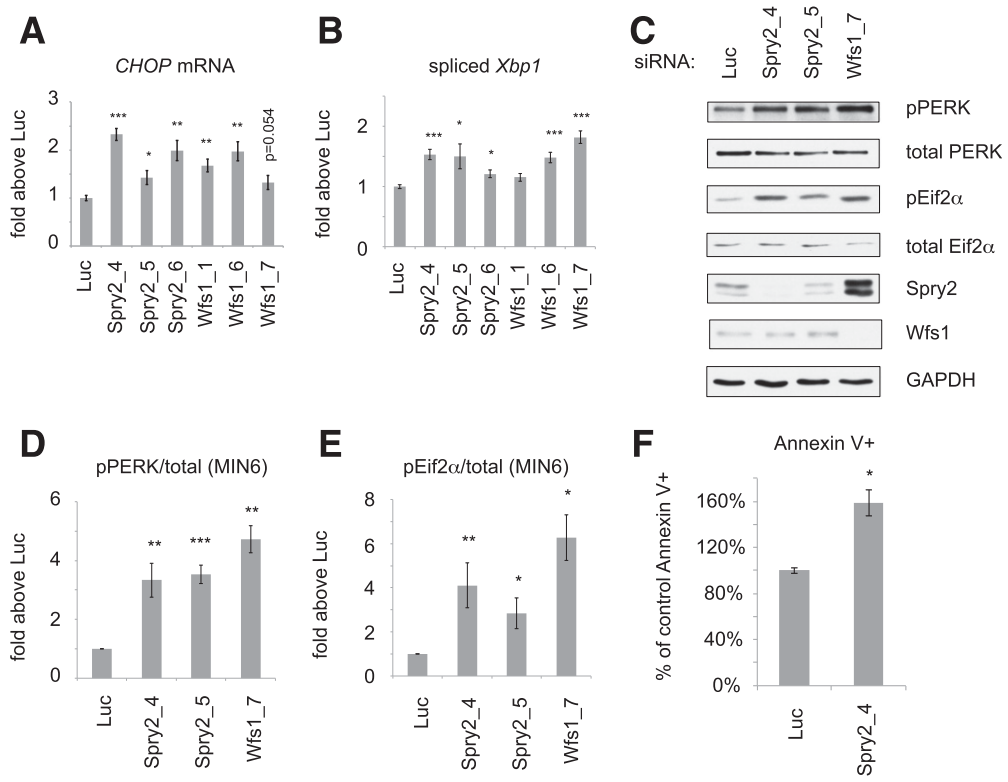

Figure 4—Knockdown of *Spry2* triggers the UPR. *A*: MIN6 cells were transfected with the indicated siRNAs, and qRT-PCR was performed for *CHOP* (n = 9). *B*: As in *A*, but for spliced *Xbp1* (n = 9). *C*: MIN6 cells were transfected with the indicated siRNAs, and Western blots were run for the indicated proteins. This is a representative blot of 3–6 experiments. *D*: Quantitation of phospho-PERK normalized to total PERK (n = 3–6). *E*: Quantitation of phospho-Eif2α normalized to total Eif2α (n = 3–6). *F*: MIN6 cells transfected with the indicated siRNAs and annexin V^+ cells were measured by flow cytometry (n = 9). SEM is plotted. *$P < 0.05$, **$P < 0.01$, ***$P < 0.001$.

in the *Spry2* β-ko as compared with β-het islets (Supplementary Fig. 7*G*), and we also did not find any difference in β-cell area in the Spry2 β-ko as compared with the Spry2 β-het mice (Supplementary Fig. 7*H*). Batch in vitro glucose-stimulated insulin secretion of islets from Spry2 β-het or Spry2 β-ko mice was also not different (Supplementary Fig. 7*I*).

β-Cell–Specific Deletion of *Spry2* Results in UPR Activation in Islets

Confirming our data in MIN6 cells, phospho-PERK levels were elevated in the islets of *Spry2* β-ko mice as compared with those from *Spry2* wt mice (Fig. 6*F* and *G*). Phospho-Eif2α levels and CHOP mRNA were also increased in *Spry2* β-ko islets, but these increases did not reach our statistical significance cutoff (P = 0.07 and P = 0.055, respectively) (Fig. 6*H* and Supplementary Fig. 8*A*). As in MIN6 cells, we did not detect differences in ATF4 in islets from Spry2 β-ko mice (Supplementary Fig. 8*B*), which suggests that it is predominantly the PERK pathway that is activated by *Spry2* loss in the β-cell. Unlike in MIN6 cells, we did not detect a difference in spliced *Xbp1* mRNA in *Spry2* β-ko islets (Supplementary Fig. 8*A*). We also did not detect a difference in fasting proinsulin levels between Spry2 β-ko and Spry2 β-het mice (Supplementary Fig. 8*C*).

DISCUSSION

We describe the first whole-genome RNAi screen for regulators of the insulin promoter. In terms of absolute insulin mRNA reduction, the strongest hits came from knockdown of the well-known transcription factors *Glis3*, *NeuroD1*, and *Pdx1*—perhaps not surprising since these proteins bind directly to the insulin promoter. Other hits were previously known to positively regulate insulin secretion in the β-cell but not insulin transcription. For example, *Gpr142* was known to positively regulate insulin secretion in vivo and in vitro, and we now identify it as a potential regulator of insulin transcription (31,32). *Gpr75* positively regulates insulin secretion in cell lines, and our data further these findings by showing that loss of *Gpr75* results in impaired insulin secretion in vivo (33). More importantly, these data show that our screen was able to identify regulators of β-cell function that are relevant in vivo. Since most of our hits have no known connection to β-cell function, the study of these novel regulators will greatly expand our understanding of insulin regulation.

On a global level, this unbiased screen highlights several critical pathways required for insulin transcription. Multiple components of the oxidative phosphorylation cascade were identified as positive regulators of

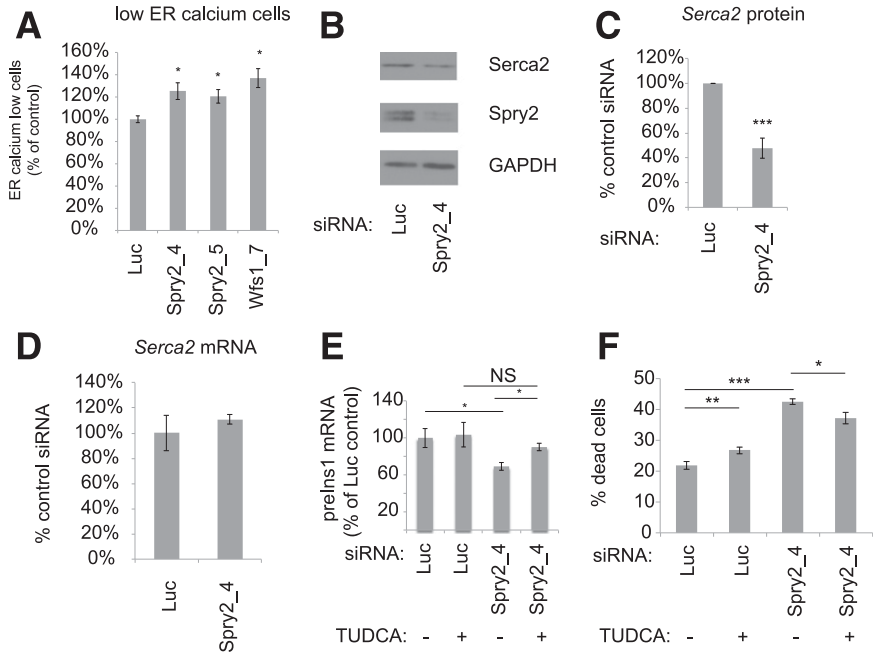

Figure 5—*Spry2* knockdown affects ER calcium. *A*: D1ER-expressing MIN6 cells were transfected with the indicated siRNAs. A total of 10,000 live events were analyzed for FRET, and the percent change in the frequency of cells with low ER calcium relative to the luciferase control is plotted (n = 7–8). *B*: MIN6 cells were transfected with the indicated siRNAs, and the indicated proteins were measured by Western blot (n = 9). *C*: Quantitation of *B*. *D*: MIN6 cells were transfected with the indicated siRNAs, and *Serca2b* mRNA was measured by qRT-PCR (n = 3). *E*: MIN6 cells were transfected with the indicated siRNAs and treated with TUDCA (500 μmol/L) or vehicle for 24 h prior to harvest. qRT-PCR for pre*Ins1* was performed (n = 3). *F*: As in *E*, but percent dead cells was quantified by flow cytometry (n = 6). SEM is plotted. *P < 0.05, **P < 0.01, ***P < 0.001.

insulin mRNA production (*Atp5a1*, *Atp5j2*, *Cox6b1*, *Cox6c*, *Cox7a2*). While oxidative phosphorylation is known to be important in glucose sensing for insulin secretion, our data suggests that it is also important for insulin transcription (34).

ER stress and the UPR were another thematic area identified by the screen. The UPR is known to reduce insulin transcription through multiple mechanisms, including ATF6 and spliced XBP1 (35–37). Besides *Wfs1*, activation of the UPR likely also explains the hits involved in vesicular trafficking between the ER and the Golgi (*Copb1, Gbf1, Sec23b*). In fact, mice lacking the small GTPase *Sec23b* lack professional secretory cells (including β-cells) and have UPR activation in the embryonic pancreas (38).

We chose to focus on *Spry2* because a SNP near the gene is associated with type 2 diabetes. We show a novel role for *Spry2* in insulin transcription and glucose homeostasis in vivo. Furthermore, we demonstrate that *Spry2* is both a target and a negative regulator of the PERK arm of the UPR, suggesting that upregulation of *Spry2* may be a part of the homeostatic response to increased ER stress. However, we were unable to detect a change in β-cell area or in in vitro insulin secretion in *Spry2* β-ko mice. Since the hyperglycemia of the *Spry2* β-ko mice was relatively mild, we might only expect a small reduction in these assays that could be below our limit of detection. Therefore, the defect in the Spry2 β-ko islets could be from reduced mass, reduced insulin secretion, or possibly both.

Our data nonetheless demonstrate an explanation of how a SNP near *Spry2* might cause human diabetes—through activation of the β-cell UPR. How could loss of *Spry2* activate the UPR? Although Spry1 and Spry2 have been previously shown to bind to and negatively regulate PLCγ1 activity in non–β-cells, thereby reducing inositol triphosphate production and calcium efflux from the ER, we did not observe changes in PLCγ1 phosphorylation or increased inositol phosphate production (39). Instead, we found that *Spry2* knockdown in β-cells causes reduced Serca2 protein levels, suggesting a possible mechanism by which *Spry2* loss might cause reduced ER calcium and the UPR. However, since ER calcium concentrations can also be reduced by high levels of ER stress, it remains possible that *Spry2* loss causes ER stress by an alternative mechanism, such as accumulation of ubiquitylated proteins, decreased autophagy, or altered vesicular traffic (20,26,40,41). Future studies will be required to define how *Spry2* loss results in activation of the UPR.

In summary, we have performed the first whole-genome RNAi screen in β-cells. We have identified novel and unexpected positive regulators of the insulin promoter and have begun to elucidate how these genes function together to control pancreatic β-cell insulin production. Specifically,

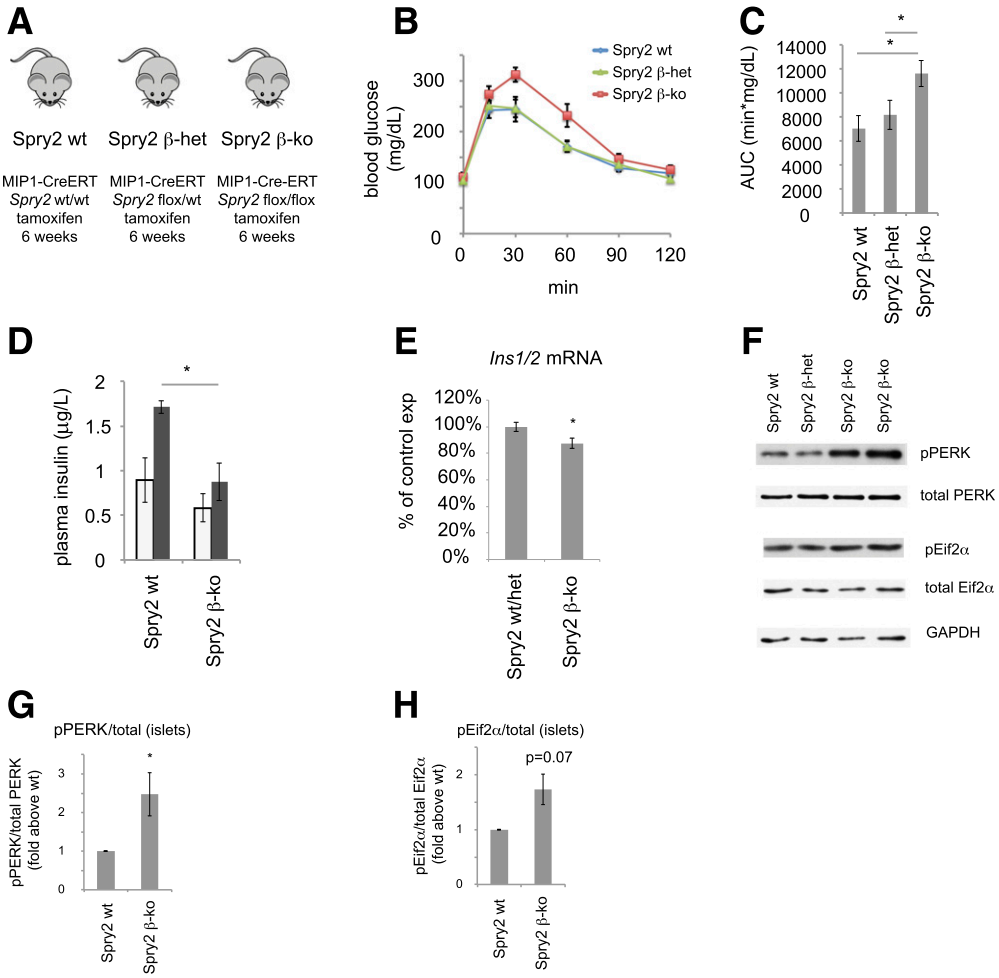

Figure 6—β-Cell deletion of *Spry2* knockdown causes hyperglycemia and hypoinsulinemia. *A*: Complete genotypes of mice used in this study. *B*: Intraperitoneal glucose tolerance testing in mice of the indicated genotypes at 12 weeks of age. $P < 0.05$ between *Spry2* wt and Spry2 β-ko ($n = 7$ wt, 11 β-het, 13 β-ko). *C*: Area under the curve (AUC) above fasting glucose for *B*. *D*: Plasma insulin levels, either fasting or 15 min after intraperitoneal glucose challenge, at 14 weeks of age ($n = 3$ *Spry2* wt, 3 *Spry2* β-ko). *E*: qRT-PCR for Ins1/2 mRNA from islets of the indicated genotypes isolated at 17 weeks of age ($n = 16$ *Spry2* wt, β-het; $n = 12$ *Spry2* β-flox). *F*: Islets from mice of the indicated genotypes were analyzed for phospho-PERK, total PERK, phospho-Eif2α, or total Eif2α. *G*: Quantitation of phospho-PERK/total PERK ($n = 4$ *Spry2* wt, 5 β-ko). *H*: Quantitation of phospho-Eif2α/total Eif2α ($n = 4$ *Spry2* wt, 5 β-ko). SEM is plotted. *$P < 0.05$. exp, expression.

we have demonstrated a novel role for *Spry2* in the UPR and in insulin production in β-cells, possibly explaining the association between SNPs near *Spry2* and type 2 diabetes susceptibility. Further understanding of the role of *Spry2* and the UPR may provide novel therapeutic inroads to understand and treat human diabetes.

Acknowledgments. The authors thank Dr. Feroz Papa (University of California, San Francisco) for useful discussion.

Funding. This work was supported by National Institutes of Health National Institute of Diabetes and Digestive and Kidney Diseases grants 5R01-DK-021344 (M.S.G.), 5RC1-DK-086290 (M.T.M.), 5K08-DK-087945 and 5R01-DK-107650 (G.M.K.), and P30-DK-087945; National Institute of Mental Health grant U01MH105028 (M.T.M.); the A.P. Giannini Foundation (G.M.K.); and JDRF grant 5-CDA-2014-199-A-N (G.M.K.).

Duality of Interest. No potential conflicts of interest relevant to this article were reported.

Author Contributions. M.S.G., M.T.M., and G.M.K. conceived of the experiments. Z.P., D.G.C., T.G.H., H.R., J.C., K.Y., L.B., K.A., S.C., M.A., and G.M.K. performed experiments, analyzed data, and reviewed the manuscript. G.M.K. wrote the manuscript. G.M.K. is the guarantor of this work and, as such, had full access to all the data in the study and takes responsibility for the integrity of the data and the accuracy of the data analysis.

Prior Presentation. Parts of this study were presented in abstract form at the 75th Scientific Sessions of the American Diabetes Association, Boston, MA, 5–9 June 2015.

References

1. International Diabetes Federation. *IDF Diabetes Atlas, 7th edition* [Internet], 2015. Available from http://diabetesatlas.org. Accessed 3 August 2016

2. Maahs DM, West NA, Lawrence JM, Mayer-Davis EJ. Epidemiology of type 1 diabetes. Endocrinol Metab Clin North Am 2010;39:481–497

3. Dabelea D, Mayer-Davis EJ, Saydah S, et al.; SEARCH for Diabetes in Youth Study. Prevalence of type 1 and type 2 diabetes among children and adolescents from 2001 to 2009. JAMA 2014;311:1778–1786

4. Morris AP. Fine mapping of type 2 diabetes susceptibility loci. Curr Diab Rep 2014;14:549
5. Imamura M, Iwata M, Maegawa H, et al. Genetic variants at CDC123/CAMK1D and SPRY2 are associated with susceptibility to type 2 diabetes in the Japanese population. Diabetologia 2011;54:3071–3077
6. Mahajan A, Go MJ, Zhang W, et al.; DIAbetes Genetics Replication And Meta-analysis (DIAGRAM) Consortium; Asian Genetic Epidemiology Network Type 2 Diabetes (AGEN-T2D) Consortium; South Asian Type 2 Diabetes (SAT2D) Consortium; Mexican American Type 2 Diabetes (MAT2D) Consortium; Type 2 Diabetes Genetic Exploration by Nex-generation sequencing in muylti-Ethnic Samples (T2D-GENES) Consortium. Genome-wide trans-ancestry meta-analysis provides insight into the genetic architecture of type 2 diabetes susceptibility. Nat Genet 2014;46:234–244
7. Shu XO, Long J, Cai Q, et al. Identification of new genetic risk variants for type 2 diabetes. PLoS Genet 2010;6:e1001127
8. Ku GM, Pappalardo Z, Luo CC, German MS, McManus MT. An siRNA screen in pancreatic beta cells reveals a role for Gpr27 in insulin production. PLoS Genet 2012;8:e1002449
9. Ku GM, Kim H, Vaughn IW, et al. Research resource: RNA-Seq reveals unique features of the pancreatic β-cell transcriptome. Mol Endocrinol 2012;26:1783–1792
10. Trapnell C, Roberts A, Goff L, et al. Differential gene and transcript expression analysis of RNA-seq experiments with TopHat and Cufflinks. Nat Protoc 2012;7:562–578
11. Huang DW, Sherman BT, Tan Q, et al. DAVID Bioinformatics Resources: expanded annotation database and novel algorithms to better extract biology from large gene lists. Nucleic Acids Res 2007;35:W169–W175.
12. Szot GL, Koudria P, Bluestone JA. Murine pancreatic islet isolation. J Vis Exp 2007;(7):255
13. Zhang JH, Chung TD, Oldenburg KR. A simple statistical parameter for use in evaluation and validation of high throughput screening assays. J Biomol Screen 1999;4:67–73
14. König R, Chiang CY, Tu BP, et al. A probability-based approach for the analysis of large-scale RNAi screens. Nat Methods 2007;4:847–849
15. Evans-Molina C, Garmey JC, Ketchum R, Brayman KL, Deng S, Mirmira RG. Glucose regulation of insulin gene transcription and pre-mRNA processing in human islets. Diabetes 2007;56:827–835
16. Iype T, Francis J, Garmey JC, et al. Mechanism of insulin gene regulation by the pancreatic transcription factor Pdx-1: application of pre-mRNA analysis and chromatin immunoprecipitation to assess formation of functional transcriptional complexes. J Biol Chem 2005;280:16798–16807
17. Eizirik DL, Sammeth M, Bouckenooghe T, et al. The human pancreatic islet transcriptome: expression of candidate genes for type 1 diabetes and the impact of pro-inflammatory cytokines. PLoS Genet 2012;8:e1002552
18. Guy GR, Jackson RA, Yusoff P, Chow SY. Sprouty proteins: modified modulators, matchmakers or missing links? J Endocrinol 2009;203:191–202
19. Khoo S, Griffen SC, Xia Y, Baer RJ, German MS, Cobb MH. Regulation of insulin gene transcription by ERK1 and ERK2 in pancreatic beta cells. J Biol Chem 2003;278:32969–32977
20. Reneker LW, Chen H, Overbeek PA. Activation of unfolded protein response in transgenic mouse lenses. Invest Ophthalmol Vis Sci 2011;52:2100–2108
21. Cnop M, Abdulkarim B, Bottu G, et al. RNA sequencing identifies dysregulation of the human pancreatic islet transcriptome by the saturated fatty acid palmitate. Diabetes 2014;63:1978–1993
22. Ueda K, Kawano J, Takeda K, et al. Endoplasmic reticulum stress induces Wfs1 gene expression in pancreatic beta-cells via transcriptional activation. *EurJ Endocrinol* 2005;153:167–176
23. Fonseca SG, Fukuma M, Lipson KL, et al. WFS1 is a novel component of the unfolded protein response and maintains homeostasis of the endoplasmic reticulum in pancreatic beta-cells. J Biol Chem 2005;280:39609–39615
24. Riggs AC, Bernal-Mizrachi E, Ohsugi M, et al. Mice conditionally lacking the Wolfram gene in pancreatic islet beta cells exhibit diabetes as a result of enhanced endoplasmic reticulum stress and apoptosis. Diabetologia 2005;48:2313–2321
25. Yamada T, Ishihara H, Tamura A, et al. WFS1-deficiency increases endoplasmic reticulum stress, impairs cell cycle progression and triggers the apoptotic pathway specifically in pancreatic beta-cells. Hum Mol Genet 2006;15:1600–1609
26. Hara T, Mahadevan J, Kanekura K, Hara M, Lu S, Urano F. Calcium efflux from the endoplasmic reticulum leads to β-cell death. Endocrinology 2014;155:758–768
27. Palmer AE, Jin C, Reed JC, Tsien RY. Bcl-2-mediated alterations in endoplasmic reticulum Ca2+ analyzed with an improved genetically encoded fluorescent sensor. Proc Natl Acad Sci U S A 2004;101:17404–17409
28. Wicksteed B, Brissova M, Yan W, et al. Conditional gene targeting in mouse pancreatic β-Cells: analysis of ectopic Cre transgene expression in the brain. Diabetes 2010;59:3090–3098
29. Shim K, Minowada G, Coling DE, Martin GR. Sprouty2, a mouse deafness gene, regulates cell fate decisions in the auditory sensory epithelium by antagonizing FGF signaling. Dev Cell 2005;8:553–564
30. Benner C, van der Meulen T, Cacéres E, Tigyi K, Donaldson CJ, Huising MO. The transcriptional landscape of mouse beta cells compared to human beta cells reveals notable species differences in long non-coding RNA and protein-coding gene expression. BMC Genomics 2014;15:620
31. Lin HV, Efanov AM, Fang X, et al. GPR142 controls tryptophan-induced insulin and incretin hormone secretion to improve glucose metabolism. PLoS One 2016;11:e0157298
32. Wang J, Carrillo JJ, Lin HV. GPR142 agonists stimulate glucose-dependent insulin secretion via Gq-dependent signaling. PLoS One 2016;11:e0154452
33. Liu B, Hassan Z, Amisten S, et al. The novel chemokine receptor, G-protein-coupled receptor 75, is expressed by islets and is coupled to stimulation of insulin secretion and improved glucose homeostasis. Diabetologia 2013;56:2467–2476
34. Prentki M, Matschinsky FM, Madiraju SR. Metabolic signaling in fuel-induced insulin secretion. Cell Metab 2013;18:162–185
35. Seo HY, Kim YD, Lee KM, et al. Endoplasmic reticulum stress-induced activation of activating transcription factor 6 decreases insulin gene expression via up-regulation of orphan nuclear receptor small heterodimer partner. Endocrinology 2008;149:3832–3841
36. Amyot J, Benterki I, Fontés G, et al. Binding of activating transcription factor 6 to the A5/Core of the rat insulin II gene promoter does not mediate its transcriptional repression. J Mol Endocrinol 2011;47:273–283
37. Allagnat F, Christulia F, Ortis F, et al. Sustained production of spliced X-box binding protein 1 (XBP1) induces pancreatic beta cell dysfunction and apoptosis. Diabetologia 2010;53:1120–1130
38. Tao J, Zhu M, Wang H, et al. SEC23B is required for the maintenance of murine professional secretory tissues. Proc Natl Acad Sci U S A 2012;109:E2001–E2009
39. Akbulut S, Reddi AL, Aggarwal P, et al. Sprouty proteins inhibit receptor-mediated activation of phosphatidylinositol-specific phospholipase C. Mol Biol Cell 2010;21:3487–3496
40. Preston AM, Gurisik E, Bartley C, Laybutt DR, Biden TJ. Reduced endoplasmic reticulum (ER)-to-Golgi protein trafficking contributes to ER stress in lipotoxic mouse beta cells by promoting protein overload. Diabetologia 2009;52:2369–2373
41. Bachar-Wikstrom E, Wikstrom JD, Ariav Y, et al. Stimulation of autophagy improves endoplasmic reticulum stress-induced diabetes. Diabetes 2013;62:1227–1237